



## Research article

# An immunoinformatics approach for a potential NY-ESO-1 and WT1 based multi-epitope vaccine designing against triple-negative breast cancer

Alima Khanam <sup>a,1</sup>, Hossain Mohammad Hridoy <sup>a,1</sup>, Md Shahin Alam <sup>b</sup>,  
Adiba Sultana <sup>b</sup>, Imtiaj Hasan <sup>a,c,\*</sup>

<sup>a</sup> Department of Biochemistry and Molecular Biology, University of Rajshahi, Rajshahi, 6205, Bangladesh

<sup>b</sup> Department of Statistics, University of Rajshahi, Rajshahi, 6205, Bangladesh

<sup>c</sup> Department of Microbiology, University of Rajshahi, Rajshahi, 6205, Bangladesh

## ARTICLE INFO

## Keywords:

Triple-negative breast cancer (TNBC)  
Cancer vaccines  
Immunoinformatics  
Multi-epitope vaccine  
Immune response  
Antigenic proteins

## ABSTRACT

Breast cancer emerges as one of the most prevalent malignancies in women, its incidence showing a concerning upward trend. Among the diverse array of breast cancer subtypes, triple-negative breast cancer (TNBC) assumes notable significance, due to lack of estrogen, progesterone, and HER-2 receptors. More focus has to be placed on creating effective therapy due to the high prevalence and rising incidence of TNBC. Currently, conventional passive treatments have several drawbacks that have not yet been resolved. On the other hand, as innovative immunotherapy approaches, cancer vaccines have offered promising prospects in combatting advanced stages of TNBC. Therefore, the main objective of this study was to utilize WT1 and NY-ESO-1 antigenic proteins in designing a multi-epitope vaccine against TNBC. Initially, to generate robust immune responses, we identified antigenic epitopes of both proteins and assessed their immunogenicity. In order to reduce junctional immunogenicity, promiscuous epitopes were joined using the suitable adjuvant (50S ribosomal L7/L12 protein) and incorporated appropriate linkers (GPGPG, AAY, and EAAAK). The best predicted 3D model was refined and validated to achieve an excellent 3D model. Molecular docking analysis and dynamic simulation were conducted to demonstrate the structural stability and integrity of the vaccine/TLR-4 complex. Finally, the vaccine was cloned into the vector pET28 (+). Thus, analysis of the constructed vaccine through immunoinformatics indicates its capability to elicit robust humoral and cellular immune responses in the targeted organism. As such, it holds promise as a therapeutic weapon against TNBC and may open doors for further research in the field.

## 1. Introduction

TNBC, making up about 15 %–20 % of all breast cancer cases globally, is distinguished by the lack of progesterone receptor (PR), estrogen receptor (ER), and human epidermal growth factor receptor 2 (HER2) [1,2]. Conventional procedures including chemotherapy, surgery, and radiation have been the only available treatment choices for triple negative breast cancer over the years.

\* Corresponding author. Department of Microbiology, University of Rajshahi, Rajshahi, 6205, Bangladesh.

E-mail addresses: [hasanimtiaz@yahoo.co.uk](mailto:hasanimtiaz@yahoo.co.uk), [imtiazbio@ru.ac.bd](mailto:imtiazbio@ru.ac.bd) (I. Hasan).

<sup>1</sup> These authors contributed equally to this study.

However, these approaches have drawbacks, including significant toxicity and limited effectiveness [3,4]. Because of genetic alterations in metastatic tumor cells, individuals with TNBC typically become resistant to hormonal and targeted therapy [5]. The development of immunotherapy in the realm of cancer has thus been prompted by this unmet therapeutic necessity.

Immunotherapy has become a prominent focus in cancer treatment, holding promise for extending patients' overall survival and enhancing their quality of life. Immune checkpoint inhibitors, adoptive T-cell therapy, and dendritic cell vaccine therapeutics have risen as noteworthy alternatives in the treatment of TNBC among these therapies. Research suggests that TNBC shows increased sensitivity to immunotherapy owing to its immunogenic tumor microenvironment (TME) [6]. Within cancer immunotherapy, multi-epitope peptide cancer vaccines emerge as a sophisticated method targeting the immune system to combat tumor cells. These vaccines accomplish this by enhancing the activity of CD4 + helper T lymphocytes (HTLs) and CD8 + cytotoxic T lymphocytes (CTLs), or by counteracting inhibitors of the immune response, thus bolstering the body's capacity to combat tumors. Therefore, it is imperative to innovate in the development of therapeutic cancer vaccines that can augment both cellular and humoral immune responses [7].

Novel cancer vaccines typically incorporate T-cell and B-cell epitopes targets derived from either tumor-specific or tumor-associated antigens [8]. The initial stage in developing a multi-epitope vaccine involves identifying appropriate antigens that are highly expressed in breast cancer. After conducting an exhaustive examination of existing literature, two highly expressed antigens, NY-ESO-1 and WT1, were chosen for vaccine formulation and design [9–12]. NY-ESO-1 (New York esophageal squamous cell carcinoma 1) is specifically detected in TNBC, and its expression stands as an independent favorable prognostic factor within breast cancer [10]. Additionally, Wilms' tumor 1 (WT1), functioning as a transcription factor, is detected in elevated levels within TNBC, where it exhibits overexpression associated with TNBC progression [11,13].

Although multi-epitope vaccines offer specific advantages, their limited ability to trigger immune responses poses a significant challenge for clinical use. To address this challenge and boost protective immunity, additional components called adjuvants can be incorporated to enhance both T-cell and B-cell responses [14]. Utilizing Toll-like receptor (TLR) agonists as adjuvants represents a strategy to enhance immune responses. These agonists originate from various microbial sources. Research has demonstrated that the TLR-4 agonist derived from *Mycobacterium tuberculosis*, among other recognized TLR agonists, exhibits potent adjuvant properties when combined with multi-epitope cancer vaccines. The TLR-4 agonist demonstrates potent immunological impacts on tumors and holds potential as an adjunct in cancer treatment [15]. This study introduces a multi-epitope vaccine targeting TNBC, devised using immunoinformatic techniques. Our focus revolved around identifying immunogenic peptides from two key antigens, WT1 and NY-ESO-1, and combining these peptides with the adjuvant TLR-4 agonist in a novel vaccine formulation to induce stronger immune responses and prolonged T-cell memory. This is the first time these antigens have been combined for vaccine development. The designed vaccine underwent analysis with multiple immunoinformatics tools to assess and confirm its effectiveness and suitability for TNBC immunotherapy.

## 2. Materials and methods

The methodology used in this study is succinctly outlined through a visual representation in Fig. 1.

### 2.1. Protein sequence retrieval

NY-ESO-1 (Accession No. CAA05908) and WT1 (Accession No. AAH32861) protein's amino acid sequences were downloaded in FASTA format from the National Center for Biotechnology Information (NCBI) Protein Database (<https://www.ncbi.nlm.nih.gov/protein>). These sequences were then subjected to a collection of computational tools to predict the most significant immunodominant epitopes.

### 2.2. Prediction of immunogenic epitopes

The Immune Epitope Database (IEDB) server (<http://tools.iedb.org/main/tcell/>) was utilized to analyze epitopes for both antigenic peptides. In order to stimulate protective cellular immunity, antigenic peptides must interact with MHC molecules. Therefore, the ANN-based web server NetMHCpan 4.1 EL (recommended epitope predictor as of September 2023) (<http://tools.iedb.org/main/tcell/>), was employed. NetMHCpan-4.1 covers more than 11 000 MHC molecules, spanning human (HLA-A, HLA-B, HLA-C, HLA-E, HLA-G), mouse (H-2), cattle (BoLA), primates (Patr, Mamu, Gogo), swine (SLA), equine (EQCA) and dog (DLA) [16]. Simultaneously, B cell epitopes that interact with antibodies were identified by the IEDB default recommended method Bepipred Linear Epitope Prediction

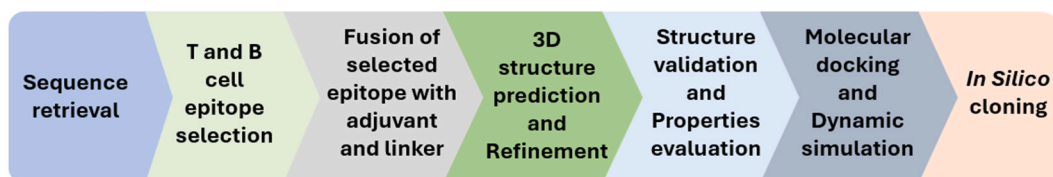


Fig. 1. The methodology of the research.

2.0 in order to promote humoral immunity. The outcomes of MHC class I and II epitope prediction for both NY-ESO-1 and WT1 proteins were expressed in percentile rank units that compares the peptide's IC<sub>50</sub> score with a randomly selected peptide set (the reference set provides a broad and unbiased baseline for comparison) from the NCBI database. The percentile rank of a peptide's IC<sub>50</sub> score is calculated by comparing it to the IC<sub>50</sub> scores of peptides in the reference set. Based on these percentile rank scores, we selected the top peptides.

### 2.3. Assessment of immunogenic properties of the predicted epitopes

Potent immunogenic peptides were chosen based on criteria such as toxicity, solubility, allergenicity, and antigenicity. The antigenic capability of the peptides was assessed using Vaxijen, a tool independent of alignment that identifies protective antigens with 85 % accuracy for tumor models, employing a threshold of 0.5 [17]. Similarly, the allergenicity, solubility, and toxicity of the generated epitopes were evaluated using AllerTop v2.0, INNOVAGEN, and ToxinPred with default settings [18–20].

### 2.4. Construction of multi-epitope vaccine sequence

The vaccine design process involved utilizing immunoinformatic tools to predict epitopes, which were then combined with adjuvants and linkers to create a complete vaccine sequence. To create a whole vaccination design, adjuvants and linkers were combined with the screened epitopes for helper T lymphocyte (HTL) epitopes, GPGPG linkers were employed, while AAY linkers were utilized for cytotoxic T lymphocyte (CTL) epitopes. The chosen adjuvant for enhancing immunogenicity was the TLR-4 agonist 50S ribosomal protein L7/L12 RplL (SA1) (Accession No. CCP43395), which was linked to both ends of the vaccine design using the EAAAK linker. Additionally, a "Histidine Tag" was incorporated at the C-terminal of the construct, connected via the RVRRL linker.

### 2.5. Epitope population coverage prediction

The frequency of different HLA genotypes varies across diverse populations globally. Using default parameters, a combined population coverage analysis of HLA classes I and II in the worldwide populations was carried out with the Immune Epitope Database (IEDB) (<http://tools.iedb.org/population/>) [21]. The frequencies for 115 countries, 21 ethnicities, and 16 geographical areas are included in this dataset. This involved inputting T-cell epitopes and their associated HLA alleles into the program. The evaluation provided diverse metrics, encompassing population coverage, epitope hits on average, and HLA combinations acknowledged by populations. It also included the minimum number of epitope combinations essential to encompass 90 % of the population (PC90).

### 2.6. Prediction of the secondary and tertiary structure

The vaccine's folding and three-dimensional form are influenced by the protein's secondary structure. Utilizing PSI-blast-based secondary structure prediction (PSIPRED), which employs two distinct feed-forward neural networks to analyze information derived from PSI-BLAST (Position Specific Iterated BLAST) [22], enables the accurate prediction of secondary structural features such as beta-sheets, alpha-helices, and turns within the amino acid sequences of the vaccine. The three-dimensional protein model of the vaccine was constructed through computational algorithms based on its amino acid sequence. In particular, the 3Dpro tool of the SCRATCH suite was utilized for this purpose [23]. This tool predicts the protein's 3D structure using iterative fragment assembly simulations and multi-threading alignments.

### 2.7. Refinement and validation of the tertiary structure

After the initial prediction of the vaccine model, refinement was performed using the GalaxyRefine webserver [24]. This webserver (<https://galaxy.seoklab.org/>) fine-tunes side chains and utilizes molecular dynamics for structural rearrangement, followed by comprehensive structural examination. GalaxyRefine stands out for its proficiency in enhancing local structural quality, as demonstrated by its performance in the CASP refinement category [25]. The best predicted model underwent validation using the SAVES v6.0 server. This server makes use of several different tools, including Verify 3D, which assesses the compatibility of an atomic model in three dimensions, ERRAT, which analyzes non-bonded atom-atom interactions, and PROCHECK, which visualizes the Ramachandran plot [26–28].

### 2.8. Analysis of immunological and physicochemical properties of vaccine

It is crucial to understand the fundamental characteristics needed to elicit a protective immune response while designing vaccines [29]. Therefore, the Vaxijen v2.0 (<https://www.ddg-pharmfac.net/vaxijen/VaxiJen/VaxiJen.html>) (accessed on February 12, 2023), ToxinPred (<https://webs.iitd.edu.in/raghava/toxinpred/protein.php>) (accessed on February 12, 2023), and AllerTop v2.0 (<https://www.ddg-pharmfac.net/AllerTOP/>) (accessed on February 12, 2023) servers were used to assess the immunological characteristics of the vaccine, including antigenicity, toxicity, and allergenicity. The constructed multi-epitope vaccine underwent physicochemical property analysis using the ProtParam web tool (<https://web.expasy.org/protparam/>) [30,31]. This tool computes a number of properties, such as half-life, grand average of hydropathicity, aliphatic index, instability index, sequence length, and molecular weight. Protein stability is evaluated using the instability index, where values less than 40 signify stability. The "N-end rule," which states that

N-terminal amino acids control protein breakdown, is the foundation for half-life prediction. The volume filled by aliphatic side chains like alanine, valine, leucine, and isoleucine is represented by the aliphatic index. Subsequently, the grand average of hydropathicity is determined by dividing the sum of hydropathy values of all residues by the total number of residues in the protein. Lastly, the vaccine was submitted to further prediction for toxicity using ToxinPred 2 (<https://webs.iitd.edu.in/raghava/toxinpred2/batch.html>) [32].

### 2.9. Docking of a designed vaccine with immune receptor TLR-4

Docking emerges as a useful method in immunoinformatics to address the issue of immune system-related protein binding prediction. The model structure was submitted to the ClusPro 2.0 server (<https://cluspro.bu.edu/login.php>) (accessed on February 12, 2023) to explore how the vaccine interacts with the TLR-4 (PDB ID: 4G8A). This server utilizes a process involving rigid body docking, which is followed by the grouping of energetically favorable structures and structural optimization steps for the docking process. Docked conformations exhibiting robust surface complementarity were selected, and their clustering characteristics were utilized for ranking [33]. Subsequently, the docked complex was visualized using PyMOL software to analyze vaccine-TLR-4 interaction, providing insights into their binding pattern. In order to investigate the binding residues between the vaccine construct and TLR-4, the complex was uploaded to the PDBsum server.

### 2.10. Molecular dynamic simulation

To examine the structural dynamics of the vaccine complex, molecular dynamics (MD) studies were carried out using the iMODS server (<http://imods.chaconlab.org/>) [34]. This tool was chosen for its rapid and efficient evaluation compared to other MD simulation servers [35]. The elastic network, covariance map, variance, eigenvalues, B-factor (mobility profiles), and deformability data are all provided by the iMODS server. Additionally, it utilizes the NAM (Nodal Analysis of Molecular dynamics) method to elucidate the collective motion of proteins in internal coordinates, making it a simple and quick tool for measuring protein flexibility [34].

### 2.11. Codon optimization and in-silico cloning

Efficiently expressing the protein in the host organism signifies the final stage in vaccine creation. The objective of this *in silico* cloning method was to anticipate the dynamics of protein expression. *Escherichia coli* K12 served as the host organism for synthesizing a codon-optimized nucleic acid sequence derived from the vaccine's amino acid sequence. This optimized sequence underwent further analysis on the JCAT server (<https://www.jcat.de/>). Subsequently, the cDNA sequence was meticulously examined using SnapGene software [36] to identify potential restriction enzyme cut sites, facilitating the digestion and cloning process of the vaccine model into the pET-28a (+) vector.

## 3. Result

### 3.1. Retrieval of protein sequence

Two proteins, NY-ESO-1 and WT1 protein were selected for this study to develop multi-epitope vaccines targeting TNBC. For analysis, we retrieved these proteins' amino acid sequences in FASTA format from the NCBI Protein Database. In our study, we use full-length proteins to ensure a comprehensive analysis and increase the likelihood of identifying all potential immunogenic peptides.

### 3.2. Prediction and screening of CTL, HTL and B-cell epitopes

Due to their major contributions to the development of long-term immunity, cytotoxic T lymphocytes (CTLs) and helper T lymphocytes (HTLs) serve as crucial elements of the adaptive immune system [37,38]. The IEDB server [39] was utilized to predict T-cell epitopes for the submitted amino acid sequences of target proteins. Initially, the analysis for NY-ESO1 revealed a total of 8344 MHC Class I epitopes and 4483 MHC Class II epitopes. In the case of WT1, the total number of MHC Class I and MHC Class II epitopes were 14 014 and 7,399, respectively. The selection of the top peptides was based on strong binders, defined by percentile rank scores, with a %rank of less than 1 for MHC Class I and less than 10 for MHC Class II. Following this, the epitopes were further narrowed down to the top 3 epitopes in both NY-ESO1 and WT1, totaling 6 epitopes for MHC I (GARGPESRL, GPRGAGAARA, TPMEAEELAR, FSRSDQLKR, RS

**Table 1**  
Anticipated MHC I binding epitopes and their immunogenic properties.

S. No	Peptides	MHC I Alleles	Vaxijen Score	Percentile rank
1	GARGPESRL	HLA- B*07:02	0.7131	0.47
2	GPRGAGAARA	HLA-B*07:02	0.9028	0.21
3	TPMEAEELAR	HLA-A*33:01	0.6434	0.93
4	FSRSDQLKR	HLA-A*31:01	1.4884	0.65
5	RSDQLKRHQ	HLA-A*31:01	1.2627	0.24
6	VRSAESETSEK	HLA-A*11:01	1.5484	0.79

DQLKRHQ and VRSASETSEK) and 6 epitopes for MHC II (TGGRGPRGAGAARAS, ASGPGGG APRGPHGG, SGPGGGAPRGPHGGA, APTLVRASSETSEKR, PTLVRASSETSEKRP and RKFSRSDHLKTHTRT) were selected for further analysis, by assessing their antigenicity, allergenicity (non-allergen), solubility (good), and toxicity (non-toxic) using AllerTop v2.0, Vaxijen 2.0, INNOVAGEN, and ToxinPred, respectively [40]. The outcome of the MHC class I and II epitope prediction for both NY-ESO-1 and WT1 are displayed in Tables 1 and 2, respectively. The rationale behind selecting specific HLA subtypes (Class I HLA: HLA-A, HLA-B, HLA-C present antigens to CD8<sup>+</sup> T cells; Class II HLA: HLA-DP, HLA-DQ, HLA-DR present antigens to CD4<sup>+</sup> T cells) for epitope prediction was to identify epitopes that can elicit robust immune reactions, strongly bind the epitopes and to ensure broad population coverage.

B-cell epitopes refer to regions on antigens where antibodies bind, eliciting an immune response. Consequently, the design of a vaccination depends primarily on the identification of these epitopes in an antigen. The IEDB server identified four B-cell epitopes for WT-1. Among them, only one epitope was antigenic, non-allergenic, and non-toxic. The epitope (SSSVKWTEGQSNHSTESDNHTTPILCGAQYRMHTHGVRFGIQDVRVPGV) with an antigenic score of 0.7600 was chosen for further analysis.

### 3.3. Assembling of multi-epitope vaccine construct

Using the proper linkers and adjuvants, the selected CTLs, HTLs, and linear B-cell epitopes were fused to generate a strong vaccine construct. Six CTL epitopes, six HTL epitopes, and a B-cell epitope totaling 392 amino acids made up the final vaccine (Fig. 2A and B). In recent decades, several TLR agonists have shown promise as vaccine adjuvants, undergoing ongoing clinical trials to assess their potential in stimulating anti-cancer immune responses. In this study, the 50S ribosomal protein L7/L12 RplL (SA1), acting as a TLR-4 agonist was employed as an adjuvant molecule positioned at the N-terminal of the vaccine using the EAAAK linker. The EAAAK linker, a rigid  $\alpha$ -helix peptide linker, effectively separates functional domains in fusion proteins. Ala-Ala-Tyr (AAY) linkers were utilized to connect the CTL epitopes, with serving as a restriction site for proteasomes in mammalian cells. Furthermore, the AAY linker enhances the immunogenicity of the vaccine construct [41]. Consequently, GPGPG linkers, known to induce HTL responses crucial for synthetic vaccines, were employed to combine CD4<sup>+</sup> epitopes [42]. B-cell peptides were then incorporated [43]. Finally, the HisTag sequence was connected in C-terminal of the vaccine construct using the RVR linker.

### 3.4. Epitope population coverage prediction

MHC or HLA molecules exhibit polymorphism, with regional variations encoding peptide-binding pathways that result in varying binding specificities. Furthermore, there are differences in the frequency of allele variations across various ethnicities. If distinct epitopes were created to cover various locations or ethnic groups, it would make things complicated [44]. Given the complexity involved, it is essential to carefully choose a potential epitope that offers extensive population coverage and strong binding capability with HLA. To evaluate the collective population frequency of the twelve T cell epitopes investigated in this study, we utilized the population coverage tool available on the IEDB interface. The selected epitopes encompass 96.66 % of the global population, as shown in both Table 3 and Fig. 3. In summary, the high percentage of population coverage provided by our proposed vaccine construct suggests its effectiveness for a vast majority of the world's population.

### 3.5. Secondary and tertiary structure prediction and refined tertiary structure validation

Secondary structures play a crucial role in the folding and overall structure of proteins [45]. The protein's predicted secondary structure as determined by the PSIPRED server is displayed in Fig. 4. According to the prediction, the protein consists of 40.05 % alpha helix (H), 7.4 % extended strand, and 42.86 % coil (C). This prediction output was subsequently employed to enhance the 3D model of the vaccine construct.

The tertiary structure prediction of the vaccine was conducted using the 3Dpro server, followed by refinement using GalaxyRefine. From GalaxyRefine, five refined structures were obtained (Table 4). Model 1 was chosen for further validation. Because, Model 1 demonstrates excellent overall structural similarity to the reference structure, evidenced by its high GDT-HA score of 0.9222, positioning it as one of the top-performing models among the five analyzed. Its low RMSD of 0.491 signifies minimal deviations from the reference structure. With a competitive MolProbity score of 1.885, Model 1 exhibits high-quality geometry and stereochemistry. Additionally, 95.9 % of its residues fall within the favored region of the Ramachandran plot, indicating superior stereochemical quality and protein geometry. Model 1 was selected for its balanced high GDT-HA score, low RMSD, and strong MolProbity and Ramachandran plot scores, making it the most reliable model among the five. The Ramachandran plot analysis of the vaccine subunit revealed that

**Table 2**  
Anticipated MHC II binding epitopes and their immunogenic properties.

S. No	Peptides	MHC II Alleles	Vaxijen Score	Percentile rank
1	TGGRGPRGAGAARAS	HLA-DQA1*05:01/DQB1*03:01	1.0671	0.26
2	ASGPGGGAPRGPHGG	HLA-DQA1*05:01/DQB1*03:01	1.1562	2
3	SGPGGGAPRGPHGGA	HLA-DQA1*05:01/DQB1*03:01	1.157	4.4
4	APTLVRASSETSEKR	HLA-DRB1*04:01	1.0625	0.96
5	PTLVRASSETSEKRP	HLA-DQA1*03:01/DQB1*03:02	1.0945	1.3
6	RKFSRSDHLKTHTRT	HLA-DRB1*11:01	1.1262	9.7

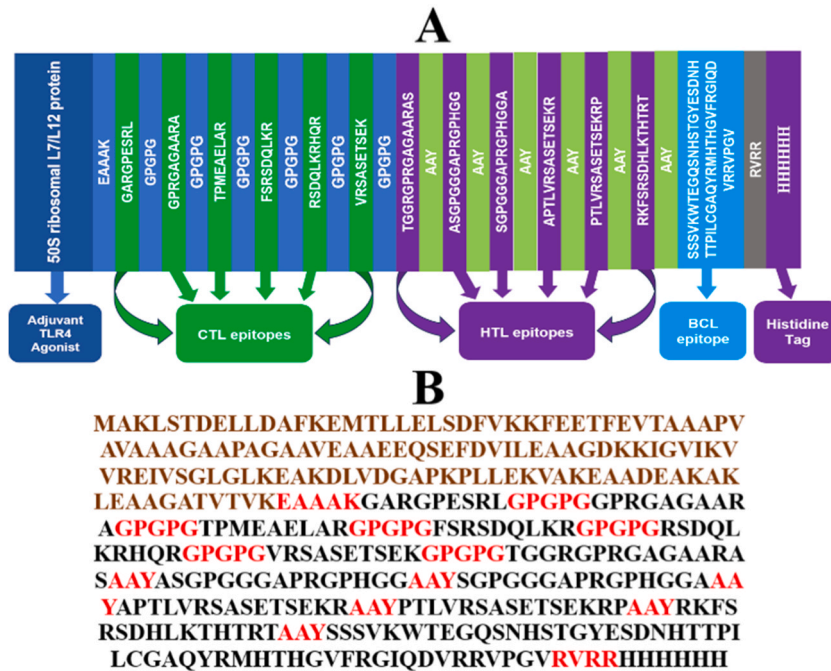


Fig. 2. (A) Schematic representation of the final multi-epitope vaccine construct. CTL—Cytotoxic T Lymphocytes; HTL—Helper T Lymphocytes; BCL—Linear B cell (B) The sequence of final novel vaccine construct.

**Table 3**  
 Combined population coverage scores for world population.

Population/area	Class combined		
	Coverage <sup>a</sup>	average hit <sup>b</sup>	pc90 <sup>c</sup>
World	96.66 %	4.89	1.87
Average	96.66 %	4.89	1.87
Standard deviation	0.0	0.0	0.0

<sup>a</sup> Projected population coverage.

<sup>b</sup> Average number of epitope hits/HLA combinations recognized by the population.

<sup>c</sup> Minimum number of epitope hits/HLA combinations recognized by 90 % of the population.

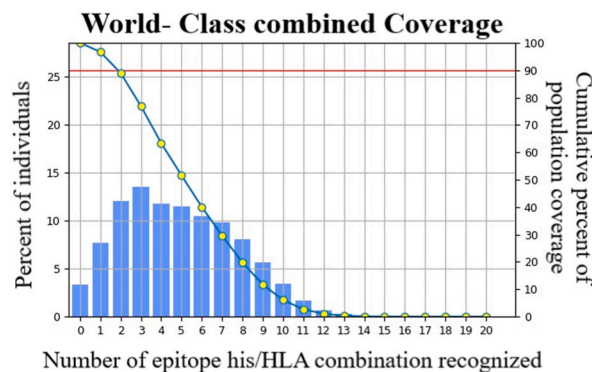


Fig. 3. Population frequency coverage analysis report of our vaccine candidate.

93.1 % of amino acid residues were situated within the favored region, with 6.3 % in the additional allowed region and only 0.3 % in the disallowed region shown in Fig. 5A, consistent with the prediction made by GalaxyRefine. This indicates the robustness and reliability of Model 1 for subsequent steps. ERRAT yields an overall quality factor of >50 for high-quality models; the quality factor of our model was 85.933 (Fig. 5B). Finally, the three-dimensional structure of the constructed vaccine was visualized using PyMOL

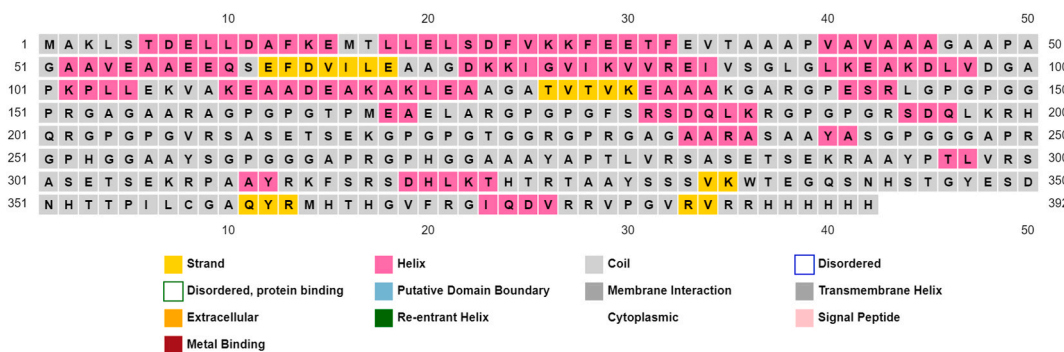


Fig. 4. Secondary structure of our vaccine candidate predicted by PsiPred chart.

Table 4

Data summary of the five refined structures.

Model	GDT-HA	RMSD	MolProbity	Rama favored
Model 1	0.9222	0.491	1.885	95.9
Model 2	0.9203	0.504	1.896	95.9
Model 3	0.9247	0.480	1.869	96.2
Model 4	0.9330	0.458	1.868	95.9
Model 5	0.9075	0.520	1.888	95.6

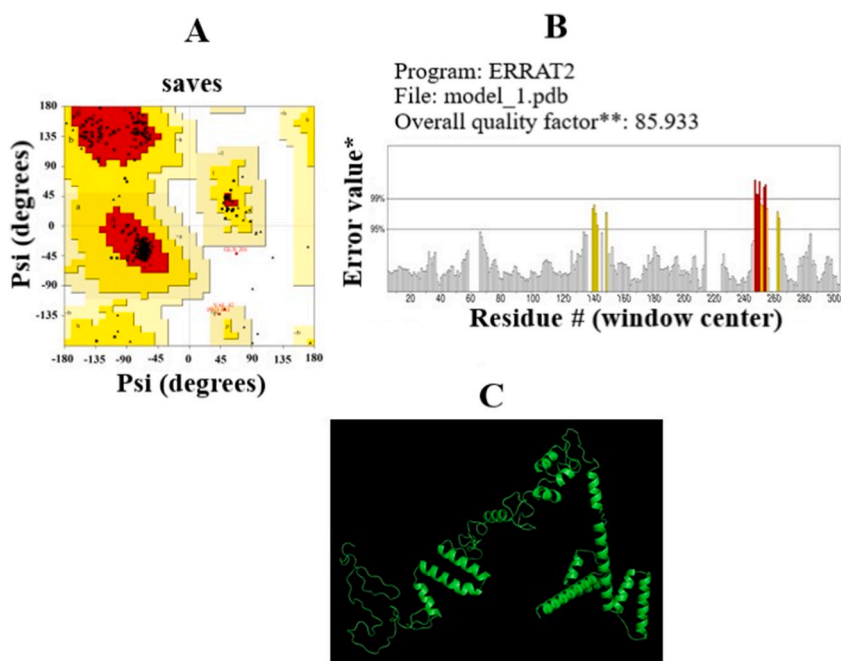


Fig. 5. Validation of the constructed vaccine model, including (A) a Ramachandran plot, residues in the most favored regions, indicated by [A, B, L], are shown in red boxes, representing the most energetically favorable conformations. Additional allowed regions [a, b, l, p] are highlighted in medium yellow boxes, while generously allowed regions [ $\sim$ a,  $\sim$ b,  $\sim$ l,  $\sim$ p] are marked with light brown boxes. Disallowed regions are shown in white, indicating conformations rarely observed due to potential steric clashes or strain; (B) an ERRAT graph, indicating \*—Error value; #—amino acid residues of the protein model. The colored bars represent the error value for amino acid residues of the protein model where red bars indicate high error values, suggesting significant inaccuracies, while yellow bars represent moderate error values, indicating potential areas of concern. (C) the modeled 3D structure of the vaccine. (For interpretation of the references to color in this figure legend, the reader is referred to the Web version of this article.)

(Fig. 5C).

### 3.6. Assessment of immunological and physicochemical properties of the construct

The newly developed vaccine underwent thorough assessment for allergenicity, toxicity, and antigenicity. An antigenicity score of 0.7200 was found, suggesting a considerable potential to initiating a potent immune response. Furthermore, the vaccine demonstrated safety with no evidence of toxicity or allergenicity, affirming its suitability for use.

In addition, the ExPASy ProtParam web server was used to analyze additional physical and chemical characteristics of the vaccine represented in Table 5. The synthesized vaccine consists of 392 amino acids and has a molecular weight of 40.23593 kDa. With an instability index of 34.37, the vaccine exhibits notable stability. Additionally, it demonstrates a high aliphatic index of 59.95 and a theoretical isoelectric point (pI) of 9.72, indicating considerable thermostability and basic nature. The vaccine design suggests a half-life of approximately 30 h in mammalian reticulocytes (in vitro), over 20 h in yeast (in vivo), and more than 10 h in *E. coli* (in vivo). Its hydrophilic protein nature, which allows it to interact with water molecules, is shown by its GRAVY (grand average of hydropathicity) score of  $-0.589$  [46]. Based on the results obtained from the ToxinPred2, it was determined that the vaccine as non-toxic.

### 3.7. Docking studies of vaccine with TLR-4

The docking outcomes revealed substantial binding of the vaccine construct to TLR-4 (with the lowest binding energy of  $-1291.8$  kcal/mol), indicating its potential efficacy, and hence, the model was taken for further analysis. The docking complex was visualized using PyMol software (Fig. 6), and interaction analysis was conducted through PDBsum. The examination focused on various binding interactions such as hydrogen bonds, salt bridges, and nonbonding contacts within the docked complexes. This analysis provided detailed insights into the amino acid residues contributing to the stability of TLR-4-vaccine complexes. The TLR-4-vaccine complex was supported by 26 salt bridges, 88 hydrogen bonds, and 777 non-bonded interactions. Details regarding the interactions exhibited by the TLR-4 molecule are listed in Table 6. The analysis revealed that nonbonded interactions predominantly contribute to the structural stability of the complex, followed by hydrogen bond interactions. The substantial number of these interacting patterns suggests a robust affinity and structural stability of the designed vaccine towards the TLR-4 receptor. The molecular interactions are shown in Supplementary Figs. 1(A–H).

### 3.8. Molecular dynamic simulation of recombinant vaccine molecule

The study utilized normal mode analysis (NMA) to evaluate both stability and global mobility of the protein complex. Fig. 7A illustrates the molecular dynamics (MD) simulation alongside the NMA of the docked complex. Deformability diagrams featured in Fig. 7B indicate regions within the designed vaccine exhibiting deformability, with peaks indicating areas of particular interest. Peaks in these diagrams represent areas with high deformability, which are flexible regions of the protein. Conversely, low peaks indicate rigid areas. Understanding these regions is crucial because flexible regions might be essential for binding and function, while rigid regions could contribute to structural stability. Furthermore, the B-factor diagram in Fig. 7C provided an average of RMS. The B-factor diagram provides an average of RMS (root mean square) fluctuations, indicating the flexibility of residues. High B-factor values suggest greater atomic displacement, signifying flexibility, while low B-factor values indicate rigidity. Dedicated values of the docked complex are detailed in Fig. 7D. In addition, the eigenvalue of  $3.475176e-07$  indicates minimal deformability of the protein complex, suggesting structural stability. In Fig. 7E presents the covariance matrix, indicating various types of motion correlations through color-coding, showing correlated motions in red, uncorrelated motions in white, and anti-correlated motions in blue. In contrast, Fig. 7F depicts the elastic network model, highlighting pairs of atoms connected by springs, with darker shades of gray indicating stiffer springs.

**Table 5**  
Physicochemical properties of the developed vaccine.

S. No	Parameters	Findings	Remark	Accepted ranges
1	No. of amino acids	392	Suitable	
2	Molecular weight	40235.93 kDa	Suitable	
3	Chemical formula	$C_{1739}H_{2789}N_{549}O_{543}S_5$	–	
4	Theoretical pI	9.72	Base	
5	Instability index	34.37	Stable	<40
6	Aliphatic index (AI)	59.95	Thermostable	AI < 70, Lower thermostability. 70 ≤ AI ≤ 85, Moderate thermostability AI > 85, More thermostable.
7	GRAVY	$-0.589$	Hydrophilic	≤ 0 [Hydrophilic]
8	Antigenicity	0.7200	Antigenic	>0.5
9	Allergenicity	No	Non-allergen	
10	Toxicity	No	Non-toxin	

GRAVY—Grand average of hydropathicity index; Theoretical pI—Isoelectric point.



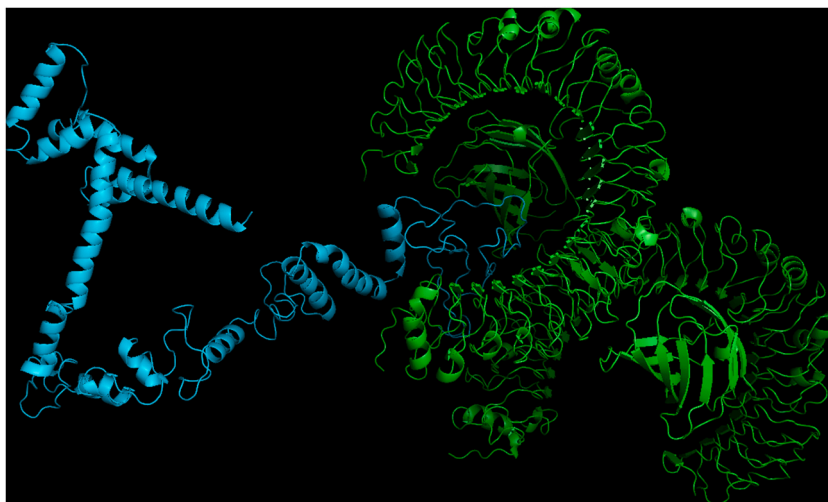


**Fig. 6.** The docking complex of the vaccine (Ligand) in blue with TLR-4 (Receptor) in green color, visualized using PyMol software. (For interpretation of the references to color in this figure legend, the reader is referred to the Web version of this article.)

**Table 6**

Interaction between different chains of TLR-vaccine complexes.

Chains	No. of salt bridges	No. of disulphide bonds	No. of hydrogen bonds	No. of non-bonded contacts
A-B	–	–	2	20
A-C	5	–	19	168
B-D	6	–	25	168
A-D	2	–	5	64
B-C	2	–	6	66
A-E	3	–	5	64
B-E	7	–	20	166
D-E	1	–	6	61

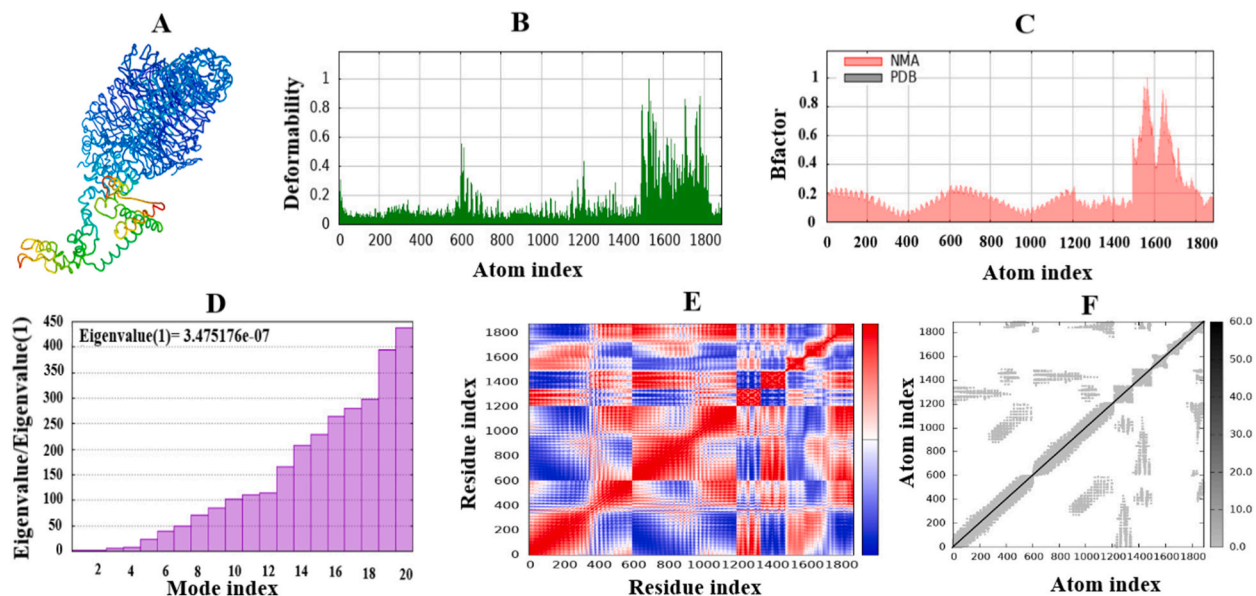


**Fig. 7.** A schematic displaying the results of the MD simulation study on the TLR-4-vaccine docked complex. Subfigures- A through F display including NMA mobility, deformability, B-factor, eigenvalues, covariance, and elastic network analysis respectively.

### 3.9. Codon optimization and in-silico cloning analysis

In order to maximize the efficiency of translation and the production yield of the recombinant product (vaccine) within the host organism (*E. coli* strain K12), the DNA sequence of the TNBC vaccine was subject to codon optimization through the CAI (Codon Adaptation Index) calculator. The resulting CAI score of 0.962 indicated the presence of favorable codons that can be effectively recognized by the cellular translation machinery of *E. coli* strain K12. A CAI score above 0.8 is generally deemed conducive. Additionally, for vaccine constructs, an optimal GC content typically falls within the range of 30–70 %. The GC content of the TNBC vaccine was determined to be 55.87 %, confirming the suitability of the sequence. Subsequently, the codon-optimized DNA sequence of the vaccine construct (Supplementary Fig. 2) was incorporated into the pET28a (+) vector, to clone it into *SgrAI* and *HpaI* restriction sites, employing the SnapGene tool. This software was utilized to introduce restriction sites at both the N and C-terminal ends of the vaccine, compensating for their absence in the original DNA sequence of the vaccine construct. The final vaccine clone, with an overall length of 1188 bp, is depicted in Fig. 8.

## 4. Discussion

With a high chance of spread and recurrence, TNBC is regarded as one of the most challenging forms of breast cancer to treat. Compared to other forms of breast cancer, TNBC has a lower survival rate. It has a high degree of malignancy, a significant invasive potential, and a short overall survival. Diagnosis often occurs at advanced stages, posing a considerable risk of visceral metastasis [47, 48]. Considering the distinctive characteristics of TNBC and the limited treatment options, immunotherapy emerges as a potential strategy for both prevention and treatment. Malignant cells that exhibit tumor antigens through MHC complexes are identified by the immune system, which is crucial in the therapy of cancer [49]. Multi-epitope vaccines aim to stimulate B and T lymphocytes to target and eliminate cancer cells. Hence, selecting suitable antigens holds crucial significance in vaccine formulation.

Prior research and clinical trials have validated the safety and efficacy of tumor antigens, NY-ESO-1 and WT1 in eliciting immune responses [50]. This study aiming to develop a novel vaccine against TNBC, we selected NY-ESO-1 and WT1 antigens. Utilizing epitopes capable of activating both B-lymphocytes and cytotoxic T lymphocytes (CTLs), along with engaging MHC-I and MHC-II molecules, is crucial in combating TNBC tumor cells. To identify the most immunogenic sequences from TNBC antigens associated with tumor progression and metastasis, we employed *in silico* tools.

Besides the crucial role of antigen selection in cancer vaccine development, the choice of adjuvant also significantly influences vaccine efficacy. Various studies have investigated different adjuvants, including aluminum salt, Montanide, and TLR agonists [51–53]. In this study, we employed a TLR-4 agonist which is well-known for its strong stimulatory qualities to enhance the immunogenicity of the newly developed construct and elicit a robust immune response. TLR-4 exhibits distinct characteristics compared to other Toll-like receptors, as it can activate both the cellular and humoral arms of the immune system simultaneously [54].

Following the selection of antigens and adjuvants, the choice of appropriate linkers is crucial for generating a protein with optimal functionality. Here, we made use of a few linkers, including AAY, GPGPG, and EAAAK. The EAAAK sequence served as a rigid linker to regulate molecular distances and minimize interference between domains [55]. Furthermore, the AAY motif aids in binding to the TAP transporter, which is essential for presenting epitopes to the immune system [56].

Several immunoinformatics servers were employed to assess the physicochemical, structural, and immunological characteristics of the designed vaccine construct. These analyses revealed an instability index of 34.37, categorizing the protein as resistant. Immunological evaluation indicated that the vaccine is non-allergenic. The performance and 3D model of the vaccine structure depend heavily on the prediction of the secondary structure. In this study, the PSIPRED server was utilized for accurate analysis of the vaccine's secondary structure displayed in Fig. 4. The biological function of the vaccine is greatly influenced by its three-dimensional structure [57]. In this study, the three-dimensional structure was validated using the SAVES v6.0 server. PROCHECK aided in visualizing the Ramachandran plot, while possible errors were found and the overall quality of the 3D model was improved using ERRAT servers. Molecular docking, a foundational technique in drug design and bioinformatics, is utilized to predict interactions between molecules like ligands and proteins, or protein-protein themselves [58]. The docking studies conducted with the ClusPro 2.0 server involve the utilization of advanced algorithms and techniques to predict the binding modes and interactions between TLR-4 and the vaccine design (Fig. 6). Furthermore, the MD simulation analyses provided substantial evidence of robust interactions between the complex. The designed vaccine demonstrates promising characteristics for stability and functionality. The deformability analysis indicates a balance between flexible regions, which are crucial for binding and function, and rigid regions, which contribute to structural stability [59]. The B-factor diagram corroborates this, showing minimal atomic displacement overall, implying a generally rigid structure [60]. The covariance matrix highlights correlated motions essential for functional conformational changes. The elastic network model reveals strong interactions between atoms, further suggesting structural stability [61]. The minimal eigenvalue of  $3.475176e-07$  indicates that the vaccine complex is highly stable with low deformability [62], that indicates the suggested vaccine can bind to immune receptors effectively and making it a strong candidate for effective vaccine development.

Codon optimization was conducted to enhance the expression levels of the novel vaccine in *E. coli* [63]. In maximizing translation efficiency and production yield of the TNBC vaccine in *E. coli* strain K12, codon optimization via the CAI calculator was performed, resulting in a favorable CAI score of 0.962. The sequence was found to be suitable following confirmation of the ideal GC content of 55.87 %. This suggests that there is a high probability of effectively overexpressing the multi-epitope vaccine in a soluble form when expressed in *E. coli*. Afterwards, SnapGene was used to incorporate the codon-optimized DNA sequence into the pET28a (+) vector (Fig. 8).

In summary, the goal of this study was to create a multi-epitope vaccine for cancer immunotherapy targeting TNBC. The vaccine

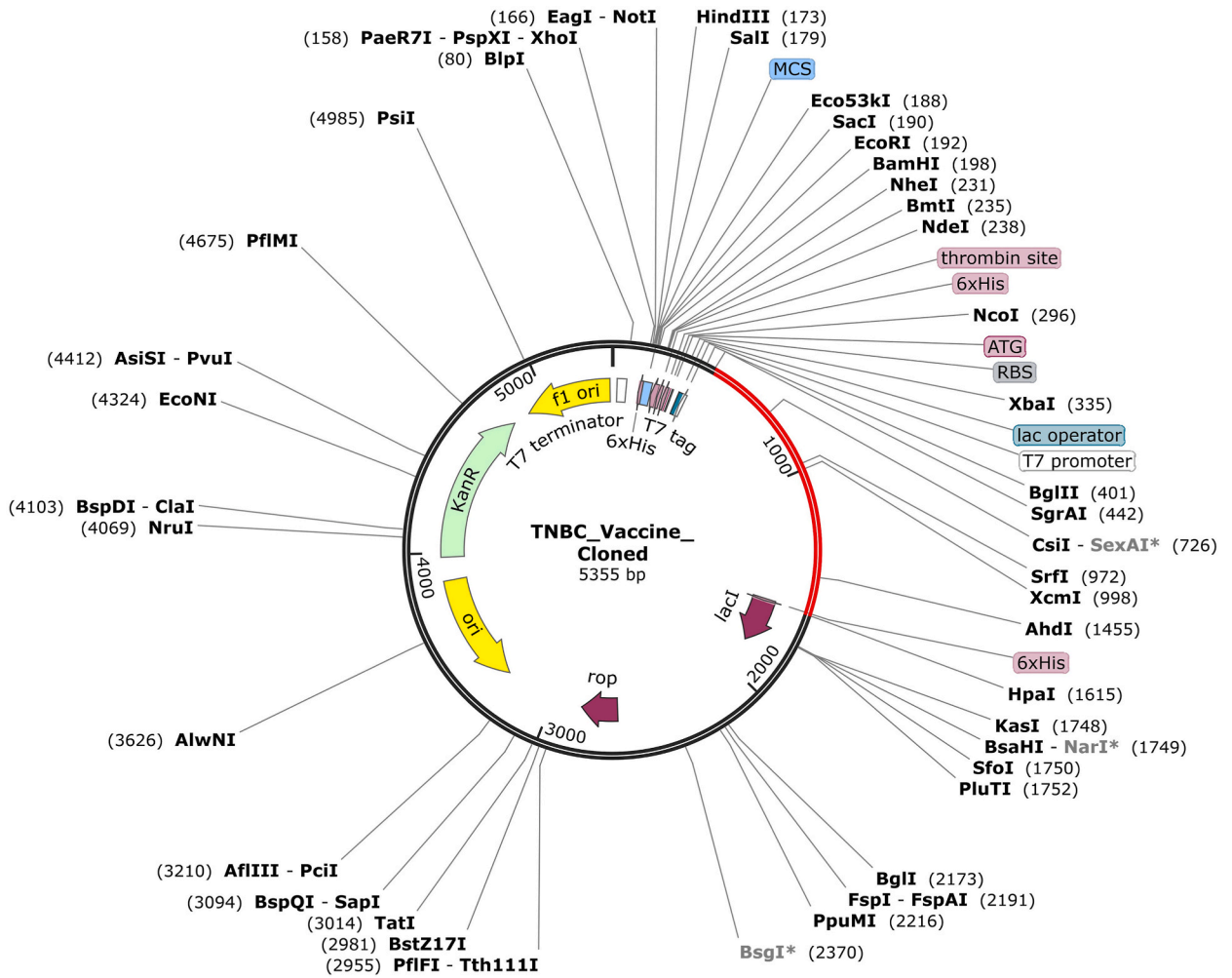


**Fig. 8.** *In silico* cloning of vaccine construct into the pET28 (+) vector using SnapGene software, (Cloned pET28a (+) vector with our vaccine construct in red). (For interpretation of the references to color in this figure legend, the reader is referred to the Web version of this article.)

design incorporated B-cell and CTL epitopes, connected by appropriate linkers to elicit both humoral and cellular immune responses. The current structure is promising due to its rational design, preliminary computational data, and target specificity. While experimental validation is yet to be conducted, the planned steps for establishing the correlation between immunoinformatic predictions and functional immunogenicity include rigorous *in vitro* and *in vivo* testing, correlation analysis, and iterative refinement. These future efforts aim to confirm the vaccine candidate’s potential for effective TNBC immunotherapy.

**5. Conclusion**

In this study, various immunoinformatic techniques were employed sequentially to develop a chimeric subunit vaccine targeting TNBC, which is associated with high mortality, recurrence, and limited treatment options. Firstly, antigenic, non-toxic, and non-allergenic epitopes for both B- and T-cells were identified from NY-ESO-1 and WT1 proteins. An efficient epitope-based peptide vaccine was produced by conjugating these epitopes with an adjuvant and linkers, which could induce both humoral and cell-mediated immunity. The vaccine’s three-dimensional model demonstrated significant interaction with TLR-4, eliciting strong cellular responses. Molecular dynamics simulations were used to further demonstrate the vaccine-TLR complex’s stability. Limitation of this study includes further validation of the proposed vaccine’s effectiveness through both *in vitro* and *in vivo* studies to confirm its immunogenic potential. These findings collectively suggest that the developed vaccine candidate holds promise for inclusion in treatment protocols for patients with TNBC, which will be an exciting avenue to take in future research.

**Ethical approval**

This is a computational study and does not involve experiments on animals or human subjects.

## Funding/support

This research did not receive any specific grant from funding agencies in the public, commercial, or not-for-profit sectors.

## Data availability statement

Data will be made available on request.

## CRediT authorship contribution statement

**Alima Khanam:** Writing – original draft, Software, Methodology, Investigation, Formal analysis, Conceptualization. **Hossain Mohammad Hridoy:** Writing – original draft, Software, Methodology, Investigation, Formal analysis, Conceptualization. **Md Shahin Alam:** Writing – review & editing, Validation, Project administration, Methodology, Investigation. **Adiba Sultana:** Writing – original draft, Validation, Methodology, Investigation. **Imtiaj Hasan:** Writing – review & editing, Validation, Supervision, Project administration, Funding acquisition, Data curation, Conceptualization.

## Declaration of competing interest

The authors declare that they have no known competing financial interests or personal relationships that could have appeared to influence the work reported in this paper.

## Appendix A. Supplementary data

Supplementary data to this article can be found online at <https://doi.org/10.1016/j.heliyon.2024.e36935>.

## References

- [1] A.G. Waks, E.P. Winer, Breast cancer treatment: a review, *JAMA* 321 (2019) 288–300, <https://doi.org/10.1001/jama.2018.19323>.
- [2] W.B. Malarkey, M. Bursleson, J.T. Cacioppo, K. Poehlmann, R. Glaser, J.K. Kiecolt-Glaser, Differential effects of estrogen and medroxyprogesterone on basal and stress-induced growth hormone release, IGF-1 levels, and cellular immunity in postmenopausal women, *Endocrine* 7 (1997) 227–233, <https://doi.org/10.1007/BF02778145>.
- [3] J. Dixon-Douglas, S. Loibl, C. Denkert, M. Telli, S. Loi, Integrating immunotherapy into the treatment landscape for patients with triple-negative breast cancer, *Am Soc Clin Oncol Educ Book* 42 (2022) 1–13, <https://doi.org/10.1200/EDBK.351186>.
- [4] X. Bai, J. Ni, J. Beretov, P. Graham, Y. Li, Immunotherapy for triple-negative breast cancer: a molecular insight into the microenvironment, treatment, and resistance, *Journal of the National Cancer Center* 1 (2021) 75–87, <https://doi.org/10.1016/j.jncc.2021.06.001>.
- [5] H. Dariushnejad, V. Ghorbanzadeh, S. Akbari, P. Hashemzadeh, Design of a novel recombinant multi-epitope vaccine against triple-negative breast cancer, *Iran. Biomed. J.* 26 (2022) 160–174, <https://doi.org/10.52547/ibj.26.2.160>.
- [6] H. Katz, M. Alsharedi, Immunotherapy in triple-negative breast cancer, *Med. Oncol.* 35 (2018) 13, <https://doi.org/10.1007/s12032-017-1071-6>.
- [7] P. Paranthaman, S. Veerappapillai, Design of a potential Sema4A-based multi-epitope vaccine to combat triple-negative breast cancer: an immunoinformatic approach, *Med. Oncol.* 40 (2023) 105, <https://doi.org/10.1007/s12032-023-01970-6>.
- [8] J.D. Fikes, A. Sette, Design of multi-epitope, analogue-based cancer vaccines, *Expert Opin Biol Ther* 3 (2003) 985–993, <https://doi.org/10.1517/14712598.3.6.985>.
- [9] G. Curigliano, V. Bagnardi, M. Ghioni, J. Louahed, V. Brichard, F.F. Lehmann, A. Marra, D. Trapani, C. Criscitiello, G. Viale, Expression of tumor-associated antigens in breast cancer subtypes, *Breast* 49 (2020) 202–209, <https://doi.org/10.1016/j.breast.2019.12.002>.
- [10] F.O. Ademuyiwa, W. Bshara, K. Attwood, C. Morrison, S.B. Edge, C.B. Ambrosone, T.L. O'Connor, E.G. Levine, A. Miliotto, E. Ritter, G. Ritter, S. Gnjatich, K. Odunsi, NY-ESO-1 cancer testis antigen demonstrates high immunogenicity in triple negative breast cancer, *PLoS One* 7 (2012) e38783, <https://doi.org/10.1371/journal.pone.0038783>.
- [11] H. Ben Haj Othmen, H. Othman, O. Khamessi, I. Bettaieb, S. Gara, M. Kharrat, Overexpression of WT1 in all molecular subtypes of breast cancer and its impact on survival: exploring oncogenic and tumor suppressor roles of distinct WT1 isoforms, *Mol. Biol. Rep.* 51 (2024) 544, <https://doi.org/10.1007/s11033-024-09450-4>.
- [12] D. Bandić, A. Juretić, B. Sarcević, V. Separović, M. Kujundžić-Tiljak, T. Hudolin, G.C. Spagnoli, D. Cović, M. Samija, Expression and possible prognostic role of MAGE-A4, NY-ESO-1, and HER-2 antigens in women with relapsing invasive ductal breast cancer: retrospective immunohistochemical study, *Croat. Med. J.* 47 (2006) 32–41.
- [13] Y. Zhang, W.-T. Yan, Z.-Y. Yang, Y.-L. Li, X.-N. Tan, J. Jiang, Y. Zhang, X.-W. Qi, The role of WT1 in breast cancer: clinical implications, biological effects and molecular mechanism, *Int. J. Biol. Sci.* 16 (2020) 1474–1480, <https://doi.org/10.7150/ijbs.39958>.
- [14] L. de Paula Peres, F.A.C. da Luz, B. dos Anjos Pultz, P.C. Brígido, R.A. de Araújo, L.R. Goulart, M.J.B. Silva, Peptide vaccines in breast cancer: the immunological basis for clinical response, *Biotechnol. Adv.* 33 (2015) 1868–1877, <https://doi.org/10.1016/j.biotechadv.2015.10.013>.
- [15] H. Dariushnejad, V. Ghorbanzadeh, S. Akbari, P. Hashemzadeh, Design of a novel recombinant multi-epitope vaccine against triple-negative breast cancer, *Iran. Biomed. J.* 26 (2022) 160–174, <https://doi.org/10.52547/ibj.26.2.160>.
- [16] B. Reynisson, B. Alvarez, S. Paul, B. Peters, M. Nielsen, NetMHCpan-4.1 and NetMHCIIpan-4.0: improved predictions of MHC antigen presentation by concurrent motif deconvolution and integration of MS MHC eluted ligand data, *Nucleic Acids Res.* 48 (2020) W449–W454, <https://doi.org/10.1093/nar/gkaa379>.
- [17] I.A. Doytchinova, D.R. Flower, VaxiJen: a server for prediction of protective antigens, tumour antigens and subunit vaccines, *BMC Bioinf.* 8 (2007) 4, <https://doi.org/10.1186/1471-2105-8-4>.
- [18] I. Dimitrov, I. Bangov, D.R. Flower, I. Doytchinova, AllerTOP v.2—a server for in silico prediction of allergens, *J. Mol. Model.* 20 (2014) 2278, <https://doi.org/10.1007/s00894-014-2278-5>.
- [19] A. Ningrum, D.W. Wardani, N. Vanidia, A. Sarifudin, R. Kumalasari, R. Ekafitri, D. Kristanti, W. Setiaboma, H.S.H. Munawaroh, In silico approach of glycinin and conglycinin chains of soybean by-product (okara) using papain and bromelain, *Molecules* 27 (2022) 6855, <https://doi.org/10.3390/molecules27206855>.

- [20] S. Gupta, P. Kapoor, K. Chaudhary, A. Gautam, R. Kumar, G.P.S. Raghava, In silico approach for predicting toxicity of peptides and proteins, *PLoS One* 8 (2013) e73957, <https://doi.org/10.1371/journal.pone.0073957>.
- [21] H.-H. Bui, J. Sidney, K. Dinh, S. Southwood, M.J. Newman, A. Sette, Predicting population coverage of T-cell epitope-based diagnostics and vaccines, *BMC Bioinform.* 7 (2006) 153, <https://doi.org/10.1186/1471-2105-7-153>.
- [22] L.J. McGuffin, K. Bryson, D.T. Jones, The PSIPRED protein structure prediction server, *Bioinformatics* 16 (2000) 404–405, <https://doi.org/10.1093/bioinformatics/16.4.404>.
- [23] J. Cheng, A.Z. Randall, M.J. Sweredoski, P. Baldi, SCRATCH: a protein structure and structural feature prediction server, *Nucleic Acids Res.* 33 (2005) W72–W76, <https://doi.org/10.1093/nar/gki396>.
- [24] J. Ko, H. Park, L. Heo, C. Seok, GalaxyWEB server for protein structure prediction and refinement, *Nucleic Acids Res.* 40 (2012) W294–W297, <https://doi.org/10.1093/nar/gks493>.
- [25] L. Heo, H. Park, C. Seok, GalaxyRefine: protein structure refinement driven by side-chain repacking, *Nucleic Acids Res.* 41 (2013) W384–W388, <https://doi.org/10.1093/nar/gkt458>.
- [26] M.E. Hodsdon, J.W. Ponder, D.P. Cistola, The NMR solution structure of intestinal fatty acid-binding protein complexed with palmitate: application of a novel distance geometry algorithm, *J. Mol. Biol.* 264 (1996) 585–602, <https://doi.org/10.1006/jmbi.1996.0663>.
- [27] C. Colovos, T.O. Yeates, Verification of protein structures: patterns of nonbonded atomic interactions, *Protein Sci.* 2 (1993) 1511–1519, <https://doi.org/10.1002/pro.5560020916>.
- [28] D. Eisenberg, R. Lüthy, J.U. Bowie, VERIFY3D: Assessment of Protein Models with Three-Dimensional Profiles, 1997, pp. 396–404, [https://doi.org/10.1016/S0076-6879\(97\)77022-8](https://doi.org/10.1016/S0076-6879(97)77022-8).
- [29] A.K. Dey, P. Malyala, M. Singh, Physicochemical and functional characterization of vaccine antigens and adjuvants, *Expert Rev. Vaccines* 13 (2014) 671–685, <https://doi.org/10.1586/14760584.2014.907528>.
- [30] V.K. Garg, H. Avasthi, A. Tiwari, P.A. Jain, P.W.R. Ramkete, A.M. Kayastha, V.K. Singh, Mfppi – multi FASTA ProtParam interface, *Bioinformatics* 12 (2016) 74–77, <https://doi.org/10.6026/97320630012074>.
- [31] M.R. Wilkins, E. Gasteiger, A. Bairoch, J.-C. Sanchez, K.L. Williams, R.D. Appel, D.F. Hochstrasser, Protein Identification and Analysis Tools in the ExPASy Server, in: 2-D Proteome Analysis Protocols, Humana Press, New Jersey, n.d.: pp. 531–552. <https://doi.org/10.1385/1-59259-584-7:531>.
- [32] N. Sharma, L.D. Naorem, S. Jain, G.P.S. Raghava, ToxinPred2: an improved method for predicting toxicity of proteins, *Brief Bioinform* 23 (2022), <https://doi.org/10.1093/bib/bbac174>.
- [33] S.R. Comeau, D.W. Gatchell, S. Vajda, C.J. Camacho, ClusPro: an automated docking and discrimination method for the prediction of protein complexes, *Bioinformatics* 20 (2004) 45–50, <https://doi.org/10.1093/bioinformatics/btg371>.
- [34] J.R. López-Blanco, J.I. Aliaga, E.S. Quintana-Ortí, P. Chacón, iMODS: internal coordinates normal mode analysis server, *Nucleic Acids Res.* 42 (2014) W271–W276, <https://doi.org/10.1093/nar/gku339>.
- [35] F. Awan, A. Obaid, A. Ikram, H. Janjua, Mutation-structure-function relationship based integrated strategy reveals the potential impact of deleterious missense mutations in autophagy related proteins on hepatocellular carcinoma (HCC): a comprehensive informatics approach, *Int. J. Mol. Sci.* 18 (2017) 139, <https://doi.org/10.3390/ijms18010139>.
- [36] K.K. Mishra, A.K. Mishra, V. Anand, A. Pandey, S. Budhwar, D.C. Sharma, Design of a multi-epitope vaccine against covid-19: an in silico approach, *Curr. Biotechnol.* 12 (2023) 151–168, <https://doi.org/10.2174/2211550112666230612153430>.
- [37] R.K. Pandey, R. Ojha, V.S. Aathmanathan, M. Krishnan, V.K. Prajapati, Immunoinformatics approaches to design a novel multi-epitope subunit vaccine against HIV infection, *Vaccine* 36 (2018) 2262–2272, <https://doi.org/10.1016/j.vaccine.2018.03.042>.
- [38] J. Maher, E.T. Davies, Targeting cytotoxic T lymphocytes for cancer immunotherapy, *Br. J. Cancer* 91 (2004) 817–821, <https://doi.org/10.1038/sj.bjc.6602022>.
- [39] Y. Kim, A. Sette, B. Peters, Applications for T-cell epitope queries and tools in the immune epitope Database and analysis resource, *J. Immunol. Methods* 374 (2011) 62–69, <https://doi.org/10.1016/j.jim.2010.10.010>.
- [40] A. Arya, S.K. Arora, A T-cell epitope-based multi-epitope vaccine designed using human HLA specific T cell epitopes induces a near-sterile immunity against experimental visceral leishmaniasis in hamsters, *Vaccines (Basel)* 9 (2021) 1058, <https://doi.org/10.3390/vaccines9101058>.
- [41] V.S. Ayyagari, T.C. V, K. A.P, K. Srirama, Design of a multi-epitope-based vaccine targeting M-protein of SARS-CoV2: an immunoinformatics approach, *J. Biomol. Struct. Dyn.* 40 (2022) 2963–2977, <https://doi.org/10.1080/07391102.2020.1850357>.
- [42] B. Livingston, C. Crimi, M. Newman, Y. Higashimoto, E. Appella, J. Sidney, A. Sette, A rational strategy to design multi-epitope immunogens based on multiple Th lymphocyte epitopes, *J. Immunol.* 168 (2002) 5499–5506, <https://doi.org/10.4049/jimmunol.168.11.5499>.
- [43] X. Li, L. Guo, M. Kong, X. Su, D. Yang, M. Zou, Y. Liu, L. Lu, Design and evaluation of a multi-epitope peptide of human metapneumovirus, *Intervirology* 58 (2015) 403–412, <https://doi.org/10.1159/000445059>.
- [44] M.S. Sakib, MdR. Islam, A.K.M.M. Hasan, A.H.M.N. Nabi, Prediction of epitope-based peptides for the utility of vaccine development from fusion and glycoprotein of niphall virus using *in silico* approach, *Adv Bioinformatics* 2014 (2014) 1–17, <https://doi.org/10.1155/2014/402492>.
- [45] A.I. Gilson, A. Marshall-Christensen, J.-M. Choi, E.I. Shakhnovich, The role of evolutionary selection in the dynamics of protein structure evolution, *Biophys. J.* 112 (2017) 1350–1365, <https://doi.org/10.1016/j.bpj.2017.02.029>.
- [46] M. Ali, R.K. Pandey, N. Khatoun, A. Narula, A. Mishra, V.K. Prajapati, Exploring dengue genome to construct a multi-epitope based subunit vaccine by utilizing immunoinformatics approach to battle against dengue infection, *Sci. Rep.* 7 (2017) 9232, <https://doi.org/10.1038/s41598-017-09199-w>.
- [47] H. Jia, C.I. Truica, B. Wang, Y. Wang, X. Ren, H.A. Harvey, J. Song, J.-M. Yang, Immunotherapy for triple-negative breast cancer: existing challenges and exciting prospects, *Drug Resist. Updates* 32 (2017) 1–15, <https://doi.org/10.1016/j.drug.2017.07.002>.
- [48] A. Papa, D. Caruso, S. Tomao, L. Rossi, E. Zaccarelli, F. Tomao, Triple-negative breast cancer: investigating potential molecular therapeutic target, *Expert Opin. Ther. Targets* 19 (2015) 55–75, <https://doi.org/10.1517/14728222.2014.970176>.
- [49] R.E. Soria-Guerra, R. Nieto-Gomez, D.O. Govea-Alonso, S. Rosales-Mendoza, An overview of bioinformatics tools for epitope prediction: implications on vaccine development, *J Biomed Inform* 53 (2015) 405–414, <https://doi.org/10.1016/j.jbi.2014.11.003>.
- [50] G. Curigliano, V. Bagnardi, M. Ghioni, J. Louahed, V. Brichard, F.F. Lehmann, A. Marra, D. Trapani, C. Criscitello, G. Viale, Expression of tumor-associated antigens in breast cancer subtypes, *Breast* 49 (2020) 202–209, <https://doi.org/10.1016/j.breast.2019.12.002>.
- [51] A.M. Didierlaurent, S. Morel, L. Lockman, S.-L. Giannini, M. Bisteau, H. Carlsen, A. Kielland, O. Vosters, N. Vanderheyde, F. Schiavetti, D. Larocque, M. Van Mechelen, N. Garcon, AS04, an aluminum salt- and TLR4 agonist-based adjuvant system, induces a transient localized innate immune response leading to enhanced adaptive immunity, *J. Immunol.* 183 (2009) 6186–6197, <https://doi.org/10.4049/jimmunol.0901474>.
- [52] C.W. Cluff, Monophosphoryl Lipid A (MPL) as an Adjuvant for Anti-cancer Vaccines: Clinical Results, 2009, pp. 111–123, [https://doi.org/10.1007/978-1-4419-1603-7\\_10](https://doi.org/10.1007/978-1-4419-1603-7_10).
- [53] N. Kayraklioglu, B. Horuluoglu, D.M. Klinman, CpG Oligonucleotides as Vaccine Adjuvants, 2021, pp. 51–85, [https://doi.org/10.1007/978-1-0716-0872-2\\_4](https://doi.org/10.1007/978-1-0716-0872-2_4).
- [54] M.S. Duthie, H.P. Windish, C.B. Fox, S.G. Reed, Use of defined TLR ligands as adjuvants within human vaccines, *Immunol. Rev.* 239 (2011) 178–196, <https://doi.org/10.1111/j.1600-065X.2010.00978.x>.
- [55] N. Nezafat, Y. Ghasemi, G. Javadi, M.J. Khoshnoud, E. Omidinia, A novel multi-epitope peptide vaccine against cancer: an in silico approach, *J. Theor. Biol.* 349 (2014) 121–134, <https://doi.org/10.1016/j.jtbi.2014.01.018>.
- [56] L.M.F. de Oliveira, M.G. Morale, A.A.M. Chaves, A.M. Cavalher, A.S. Lopes, M. de O. Diniz, A.S. Schanoski, R.L. de Melo, L.C. de S. Ferreira, M.L.S. de Oliveira, M. Demasi, P.L. Ho, Design, immune responses and anti-tumor potential of an HPV16 E6E7 multi-epitope vaccine, *PLoS One* 10 (2015) e0138686, <https://doi.org/10.1371/journal.pone.0138686>.
- [57] S.-C. Han, H.-C. Guo, S.-Q. Sun, Three-dimensional structure of foot-and-mouth disease virus and its biological functions, *Arch. Virol.* 160 (2015) 1–16, <https://doi.org/10.1007/s00705-014-2278-x>.
- [58] B.S.P.D. Schneidman-Duhovny, B.S.P.R. Nussinov, B.S.P.H.J. Wolfson, Predicting molecular interactions in silico: II. Protein-protein and protein- drug docking, *Curr. Med. Chem.* 11 (2004) 91–107, <https://doi.org/10.2174/0929867043456223>.

- [59] T.B. Mamonova, A.V. Glyakina, O.V. Galzitskaya, M.G. Kurnikova, Stability and rigidity/flexibility—two sides of the same coin? *Biochimica et Biophysica Acta (BBA) - Proteins and Proteomics* 1834 (2013) 854–866, <https://doi.org/10.1016/j.bbapap.2013.02.011>.
- [60] Z. Sun, Q. Liu, G. Qu, Y. Feng, M.T. Reetz, Utility of B-factors in protein science: interpreting rigidity, flexibility, and internal motion and engineering thermostability, *Chem Rev* 119 (2019) 1626–1665, <https://doi.org/10.1021/acs.chemrev.8b00290>.
- [61] L. Orellana, M. Rueda, C. Ferrer-Costa, J.R. Lopez-Blanco, P. Chacón, M. Orozco, Approaching elastic network models to molecular dynamics flexibility, *J Chem Theory Comput* 6 (2010) 2910–2923, <https://doi.org/10.1021/ct100208e>.
- [62] J.E. Jimenez-Roldan, R.B. Freedman, R.A. Römer, S.A. Wells, Rapid simulation of protein motion: merging flexibility, rigidity and normal mode analyses, *Phys. Biol.* 9 (2012) 016008, <https://doi.org/10.1088/1478-3975/9/1/016008>.
- [63] S.C. Makrides, Strategies for achieving high-level expression of genes in *Escherichia coli*, *Microbiol. Rev.* 60 (1996) 512–538, <https://doi.org/10.1128/mr.60.3.512-538.1996>.